SAND2019-11669C

Force Reconstruction at Mechanical Interfaces

Deborah Fowler (UMass Lowell), Samuel Parker (University of Texas at Austin), Matthew Cleal (University of New Mexico), Peter Avitabile (UMass Lowell), Patrick Logan (UMass Lowell), Daniel Roettgen (Sandia National Laboratories*), Benjamin Pacini (Sandia National Laboratories*), Robert Kuether (Sandia National Laboratories*)

ABSTRACT

Traditional approaches to analyzing nonlinear systems often involve assuming a specific model form and model order for the nonlinearity. These nonlinearities in a system could instead be modeled as a nonlinear force applied to an underlying linear system. Force reconstruction methods can be used to recreate this nonlinear force from measured data, allowing the system change to be quantified. A modal based force reconstruction technique has proven capable of recreating force inputs at unmeasured locations and has been successfully applied to nonlinear intermittent contact forces in previous studies. To extend these findings, a two-beam system was designed such that intermittent contact occurs near the joint locations and the impact forces are measured using integrated force gages. Acceleration responses are obtained from a sparse measurement grid which does not include the contact locations. The responses are used in the force reconstruction process to form estimates of the nonlinear contact forces, which are then compared to the measured force values to validate the accuracy of the results.

Keywords: force reconstruction, input localization, modal filters, equivalent loading, contact nonlinearity

* Sandia National Laboratories is a multimission laboratory managed and operated by National Technology and Engineering Solutions of Sandia, LLC., a wholly owned subsidiary of Honeywell International, Inc., for the U.S. Department of Energy's National Nuclear Security Administration under contract DE-NA-0003525.

INTRODUCTION

Many engineering structures are comprised of components connected using bolted joints. Bolted joints often have a nonlinear effect on the dynamics of a structure, as the damping and stiffness can change proportional to the vibrational amplitude [1]. A variety of methods have been developed to model and characterize the effect of joints on a structure. Phenomenological models (including Coulomb friction models) are often used due to their simplicity, but for some applications these models are not detailed enough. Constitutive contact models can be used to describe local frictional contact, though they are inherently more complex [2, 3]. Some modeling techniques characterize the nonlinear joint effects using a single element (such as an Iwan element) connected to an area representing the bolted contact region, while others model contact as node-to-node [4, 5]. These methods often incorporate experimental data by fitting the observed behavior and obtaining parameter values that can then be used in the nonlinear elements [3, 4, 5]. While these techniques produce accurate and reliable models, the assumptions underlying their development may not be appropriate for every joint or structural analysis. For this work, the effect of a nonlinear joint on a structure is regarded as an equivalent force acting on the underlying linear system. Force reconstruction techniques can then be used to locate and estimate these equivalent forces in order to quantify the nonlinear effects of the joint that are not captured in the linear model. This methodology would allow for quantification of the nonlinear effects without assumption of model order or the nature of the nonlinearity.

Previous work conducted by Zhang, Allemang, and Brown [6] and later extended by Logan and Avitabile [7, 8, 9] has proposed a force reconstruction technique which utilizes a singular value decomposition of the estimated modal forces in the frequency domain to localize inputs. Logan, Fowler and Avitabile [8] demonstrated that the technique can be used to quantify system changes and nonlinear applied loads. Previous work with this technique assumes the applied loads to be uncorrelated. While this assumption is appropriate for many applications, the equivalent forces resulting from a nonlinear joint are internal to the characterized system, which indicates multiple correlated forces. To extend this force reconstruction technique to jointed structures, modifications to the technique are necessary.

To develop these modifications, a two-beam structure was designed to exhibit similar phenomena to the nonlinearities inherent in jointed structures. The structure includes mechanical interfaces that exhibit nonlinear gap contact, with the interfacial contact forces measured by integrated force gages. These nonlinear forces are inherently correlated as the contacting beams result in equal and opposite internal forces. This paper details the modifications and additional assumptions necessary to the

force reconstruction process to accommodate these correlated forces. A set of analytical cases will be presented, followed by experimental validation using the structure's integrated force gages to confirm the technique's accuracy. Additional cases will be presented using preloaded connections to show the applicability of the technique to potentially identify bolt loosening in a jointed structure.

THEORETICAL BACKGROUND

Force Reconstruction

This section will provide a detailed overview of the force reconstruction process employed in this work, which builds on the work presented by Logan in [7, 8, 9]. The response, *X,* of a linear system to an input, *F*, where the system is characterized by a matrix of frequency response functions (FRFs), [H], at any spectral line $j\omega$, can be expressed as

$$\{X(j\omega)\} = [H(j\omega)]\{F(j\omega)\} \tag{1}$$

From a theoretical perspective, the input force can be reconstructed by an inversion of the FRF matrix as

$$\{F(j\omega)\} = [H(j\omega)]^{\dagger}\{X(j\omega)\} \tag{2}$$

where the superscript $\dagger$ represents the pseudo-inverse, or the standard inverse where the matrix is square and nonsingular.

From a practical perspective, the inversion suffers from ill-conditioning and is heavily affected by perturbation of the data. The ill-conditioning of the FRF matrix may be abated through a truncation of modes and careful selection of the physical degrees of freedom (DOFs) represented in the matrix. Reducing to *i* input DOFs and *o* response DOFs over *m* modes permits the FRF matrix to be written as

$$[H_{o,i}(j\omega)] = [U_{o,m}][\bar{H}_m(j\omega)][U_{i,m}]^T + [R_{o,i}(j\omega)] \tag{3}$$

where [U] denotes the matrices of mode shape coefficients (scaled to unit modal mass) associated with the selected modes and DOFs, $[\bar{H}]$ is a diagonal matrix of FRFs for the uncoupled modal oscillators and [R] is a matrix of residual terms not contained in the retained modes. The matrix of residuals may be considered negligible when the physical response is comprised mostly of the response of the *m* retained modes. Where acceleration measurements are employed, the FRF for the i^{th} modal oscillator is obtained from the natural frequency, $\omega_{n,}$ and modal damping, ζ, as

$$\bar{H}_i(j\omega) = \frac{-\omega^2}{\omega_{n,i}^2 - \omega^2 + 2j\zeta_i\omega_{n,i}\omega} \tag{4}$$

Modal response coordinates *p* may be estimated from the physical coordinates as

$$\{p(j\omega)\} = [U_{o,m}]^{\dagger}\{X(j\omega)\} \tag{5}$$

Modal domain force may be estimated from modal coordinates as

$$\{\bar{F}_m(j\omega)\} = [\bar{H}_m(j\omega)]^{-1}\{p(j\omega)\} \tag{6}$$

To characterize the applied forces, an *m*-by-*k* matrix of the *m* modal forces may be assembled over *k* spectral lines (with $m \leq k$) and decomposed via singular value decomposition as

$$[U_\Sigma][\Sigma][V]^T = \left[\left\{ \bar{F}_m(j\omega_1) \right\} \quad \cdots \quad \left\{ \bar{F}_m(j\omega_k) \right\} \right] \tag{7}$$

where [V] is a *k*-by-*k* unitary set of basis vectors related to frequency content, [U_Σ] is an *m*-by-*m* unitary set of basis vectors related to the modal coefficients of the input DOFs, and [Σ] is a diagonal matrix which describes the number of independent sources, or principal force components. Interrogation of the singular values permits selection of a subset of vectors of the [U_Σ] matrix, where the retained vectors are associated with the largest singular values. The retained vectors exist as a truncated basis, [U_Σ*], which approximately define the space of the estimated modal forces. The modal coefficients associated with any physical DOF may be projected, as a vector, onto the truncated basis and compared with the original coefficients. If the projection is similar to the original modal coefficients, the modal coefficients may be said to exist within the space defined by the truncated basis. The associated DOF is compatible with the estimated modal forces, such that an input applied at the DOF may produce some or all of the observed response, without also providing additional unrelated response. Alternatively, if the projection is dissimilar to the original modal coefficients, then the associated DOF is incompatible with the estimated modal forces. Input applied at an incompatible DOF will provide some response which is not related to the observed response. Figure 1 depicts the process, starting with the composition of modal forces from physical forces and mode shapes, and ending with the primary locator function, or localization function, which is used to evaluate the compatibility of each physical DOF with the estimated modal forces.

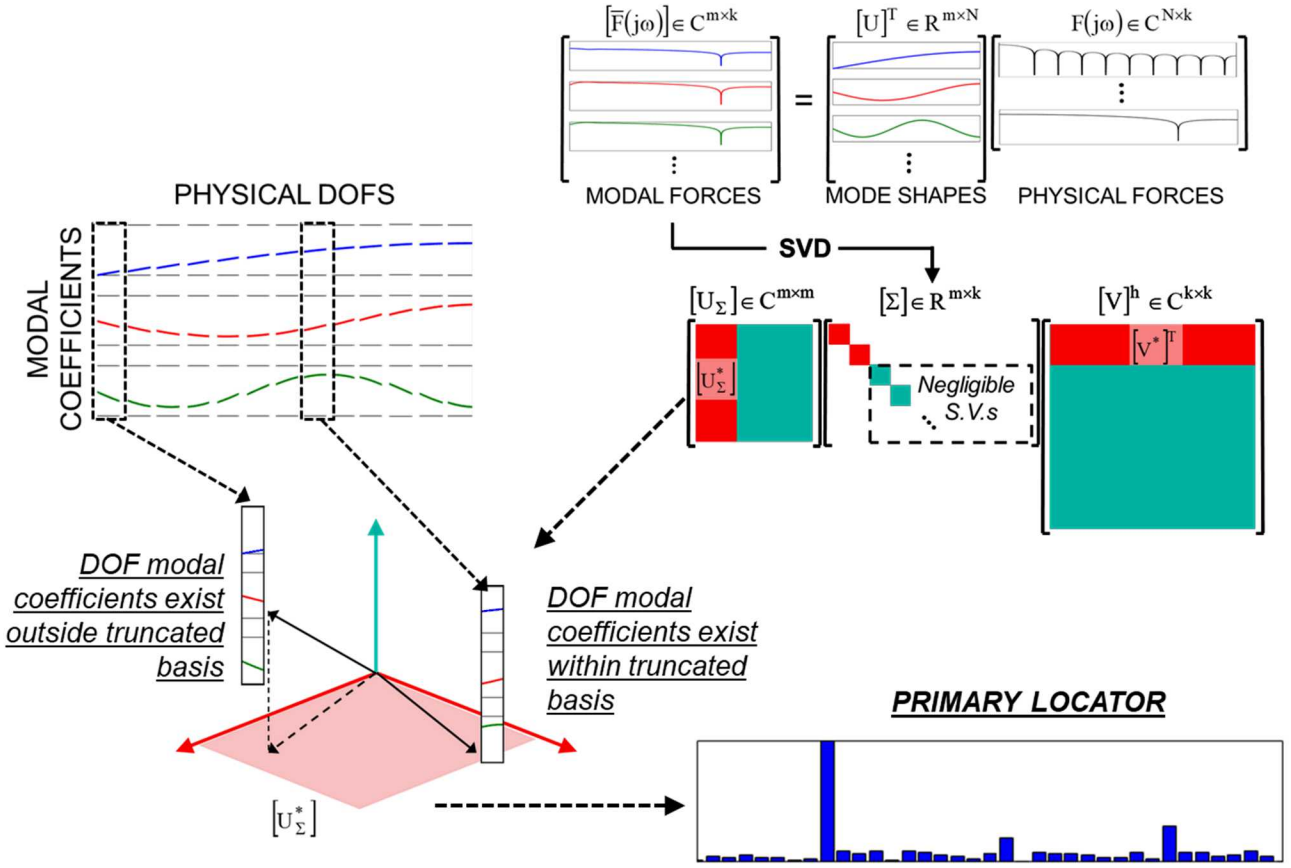

Figure 1. Modal forces, synthesized from physical inputs and modal coefficients, may be decomposed to determine the number of independent sources and the associated truncated sets of singular vectors, which may be used to develop a locator function using the modal coefficients of any number of degrees of freedom.

The primary locator, *PL*, is constructed from the truncated basis, and the mode shape coefficients of any set of *N* physical degrees of freedom. The value of the j^{th} degree of freedom is computed as

$$PL_j = \frac{\left| \left(\left[U_\Sigma^* \right] \left[U_\Sigma^* \right]^\dagger \left[U_{j,m} \right]^T \right)^h \left[U_{j,m} \right]^T \right|^2}{\left(\left(\left[U_\Sigma^* \right] \left[U_\Sigma^* \right]^\dagger \left[U_{j,m} \right]^T \right)^h \left[U_\Sigma^* \right] \left[U_\Sigma^* \right]^\dagger \left[U_{j,m} \right]^T \right) \left(\left[U_{j,m} \right] \left[U_{j,m} \right]^T \right)} \tag{8}$$

where † indicates the pseudo-inverse and the superscript *h* indicates the conjugate transpose. The localization function may be used for any number of physical degrees of freedom, including the DOFs of a well-correlated finite element model, regardless of sensor placement. The function outputs values from 0 to 1, with higher values indicating higher compatibility between a particular DOF and the estimated modal forces. Figure 2 depicts the input identification process starting from physical responses caused by an unknown input.

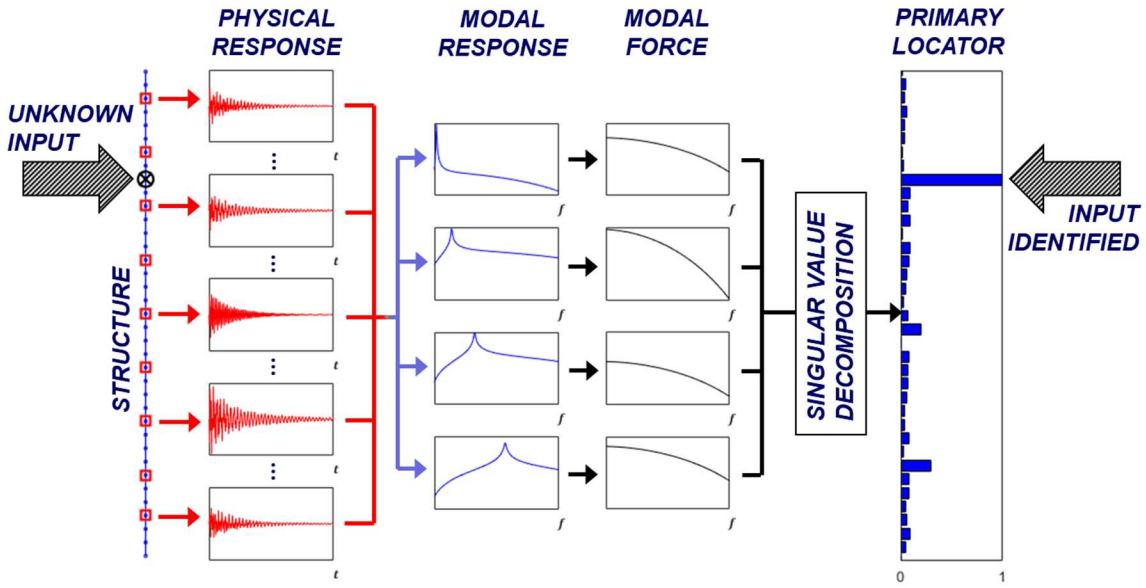

Figure 2. Process for input identification from responses caused by an unknown input.

Once physical input DOFs are identified, the estimation process is completed by transforming the modal forces to physical space as

$$\left\{ \mathrm{F_i}(\mathrm{j}\omega) \right\} = \left\{ \left[\mathrm{U_{i,m}} \right]^{\mathrm{T}} \right\}^\dagger \left\{ \mathrm{\overline{F}_m}(\mathrm{j}\omega) \right\} \tag{9}$$

In prior studies, the primary locator function correctly identified the location of a nonlinear gap contact condition at a single node of a component [8]. The contact occurred between the component of interest and a secondary component which contained no measurement points and was not considered in the reconstruction. Additionally, no coupling between the components was considered. As a result, the physical changes imposed by the secondary component were able to be characterized as a single force acting on the primary component, with effects visible in the response measurements. For the studies described within this work, the system of interest consists of two coupled components which are both considered in the reconstruction process. Each instance of inter-component contact produces a pair of forces which act on opposite components and are expected to be equal and opposite in sense, and thus, correlated. Figure 3 shows a representation of the two scenarios.

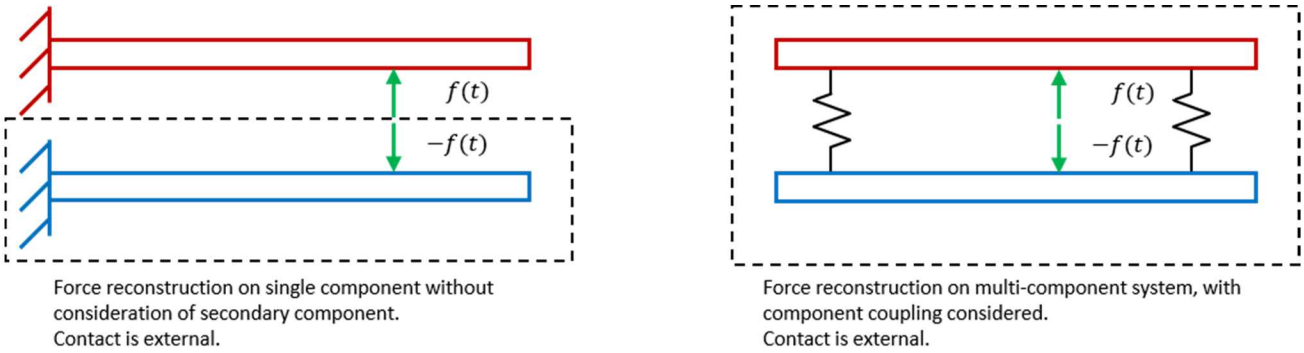

Figure 3. Comparison of external contact addressed in [8] and internal contact resulting in correlated forces.

The development of the primary locator involves the assumption that all applied forces are uncorrelated, further discussed in [9]. To modify the force reconstruction process to accommodate correlated forces additional assumptions are necessary. For the structure studied in this paper, the correlated forces in question may be considered as a single forcing function which is applied to a pair of nodes, with one node on each component. The combined modal force resulting from the pair may be expressed as

$$\left\{\bar{F}\left(j\omega\right)\right\} = \left[\frac{U^A}{U^B}\right]^T \begin{Bmatrix} F\left(j\omega\right) \\ -F\left(j\omega\right) \end{Bmatrix} \tag{10}$$

where the U^A denotes the modal coefficients of one degree of freedom of the first component, component A, and U^B denotes the modal coefficients of the contacting degree of freedom on the second component, component B. Eq. (10) may be alternatively expressed as

$$\left\{\bar{F}\left(j\omega\right)\right\} = \left(\left[U^A\right]^T - \left[U^B\right]^T\right)\left\{F\left(j\omega\right)\right\} \tag{11}$$

so that the two correlated contact forces are regarded as a single force, which is assumed to be uncorrelated to any other forces acting on the system. The difference in mode shape coefficients is used in the locator function described in Eq. (8) in place of the standard mode shape values, $U_{j,m}$. The resulting function may be termed a composite locator function, which combines the modal coefficients of the various degrees of freedom according to one or more assumptions. For this study, the composite locator function employed is intended to identify the pair of input degrees of freedom that would result in the modal forces estimated.

The mode shape difference matrix is calculated as

$$\left[\Delta U\right] = \left[U^A\right] - \left[U^B\right] \tag{12}$$

For a general contact condition, the difference matrix of Eq. (12) would include all pairs of degrees of freedom which may provide contact with each other. The composite locater, *CL*, is then computed as

$$CL_j = \frac{\left|\left(\left[U_\Sigma^*\right]\left[U_\Sigma^*\right]^\dagger\left[\Delta U_{j,m}\right]^T\right)^h\left[\Delta U_{j,m}\right]^T\right|^2}{\left(\left(\left[U_\Sigma^*\right]\left[U_\Sigma^*\right]^\dagger\left[\Delta U_{j,m}\right]^T\right)^h\left[U_\Sigma^*\right]\left[U_\Sigma^*\right]^\dagger\left[\Delta U_{j,m}\right]^T\right)\left(\left[\Delta U_{j,m}\right]\left[\Delta U_{j,m}\right]^T\right)} \tag{13}$$

where the subscript *j* now denotes a pair of degrees of freedom. With this assumption, the composite locator function can be used to locate the correlated input forces associated with contact forces that apply equal and opposite forces at internal contacting points in the structures and is demonstrated both analytically and experimentally in the sections that follow. The

resulting input degrees of freedom locating using the primary locator (for uncorrelated forces) and the composite locator (for correlated forces) are then combined in Eq. (9) to for the force estimation process.

Correlation Tools

The Modal Assurance Criterion (MAC) is a vector correlation tool used to quantify the similarity between mode shape vectors [10]; the formulation here assumes real vectors. The MAC is bounded between zero and one, with values near one indicating very similar modal vectors. The MAC is calculated using:

$$MAC_{ij} = \frac{\left[\{u_i\}^T \{e_j\}\right]^2}{\left[\{u_i\}^T \{u_i\}\right]\left[\{e_j\}^T \{e_j\}\right]} \tag{14}$$

The Pseudo Orthogonality Check (POC) is a vector correlation tool that utilizes mass scaling in the correlation process [10]. Similar to a MAC, values closer to 1 indicate high correlation. The POC is formulated as

$$POC = [U_a]^T [M_a][E_a] = [U_a]^g [E_a] \tag{15}$$

Both MAC and POC will be used to compare the mode shapes of the finite element model to the test mode shapes and to compare the expanded shapes to the measured shapes. To compare time response, a time response assurance criterion, or TRAC, is used. A TRAC is simply a MAC except that the vectors are time histories rather than mode shapes. A frequency response assurance criterion, or FRAC, is used to compare frequency vectors in the same way. Similar to a MAC, a TRAC or FRAC value near one indicates two time histories are very similar.

STRUCTURE DESCRIPTION

Figure 4 shows the test structure and a close-up of the mechanical interface. The test structure consisted of two 6061 aluminum beams 35.75 inches long and 4 inches wide, with thicknesses of ½ inch for the top beam and 5/8 inch for the bottom beam. The two beams each had twelve through-holes, allowing them to be connected by ½ inch threaded bolts. Cap nuts were used to secure the joints in order to minimize frictional contact and reduce the nonlinearities of bolted connections. Nonlinear contact points were created at each corner of the beams using a set screw and a force gage that permitted intermittent gap contact. The force gage allowed for direct measurement of the nonlinear force applied, and the set screw allowed for control of the gap distance. The structure was suspended by bungie cords to approximate a free-free boundary condition. A combination of 23 uniaxial accelerometers and 4 triaxial accelerometers were applied to the two beams for acquisition of response data. Acquisition was performed using LMS Test.Lab. The structure was excited using a modal shaker for nonlinear tests and an impact hammer for linear testing.

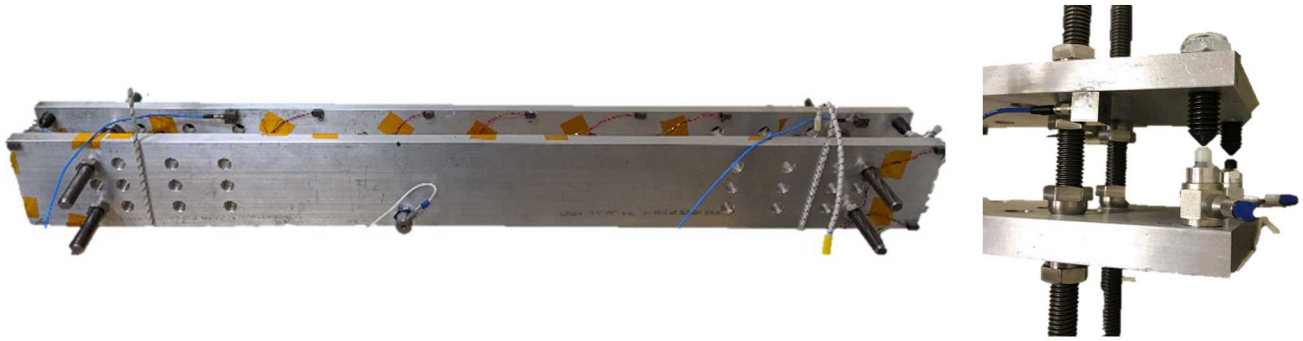

Figure 4. Test structure comprised of two aluminum beams (left) connected with threaded rods and cap nuts, with a nonlinear mechanical interface (right).

MODEL DESCRIPTION

A finite element model of the structure was developed for use in the analytical case studies, experimental force reconstruction process, and sensor selection procedures. The model represented each beam using 2501 plate elements with a node spacing of 0.125" around the joint locations and 0.25" for the remainder of the model. The plate elements used the material properties for 6061 aluminum. The rods connecting the plates were modeled using steel Euler-Bernoulli beam elements, with larger diameter beam elements to represent the cap nuts and smaller diameter beam elements to represent the rods. Point masses connected to rigid elements were used to represent the mass and location of the force gages and set screws. Soft springs attached to fixed nodes were used as boundary conditions. Figure 5 shows the finite element model of the test structure.

Figure 5. Finite element model of the test structure.

The connection between the beam and plate elements were represented at the joint locations with two methods that were used to produce two different models, shown in Figure 6. The first method directly connected the beam elements to a plate element node, with thin beam elements coupling the in-plane rotational degree of freedom. The second method used a set of rigid elements to connect the beam element to the plate element nodes, covering an area of plate elements corresponding to the area of the cap nut connection. The second method provided mode shapes that correlated better for test modes 4, 9, 11, 12, and 13. For the modal filtering process and the calculation of the primary locator function, the modes can be from different models with the primary goal being that the modes are the most accurate representation of the test structure's dynamics. The best correlated shapes from each model were used for the force reconstruction process. The correlation for the chosen set of modes is shown in

Table 1. Experimental mode 10 is poorly excited due to the motion being primarily in-plane, and so the mode was excluded from the modal filtering and force reconstruction process.

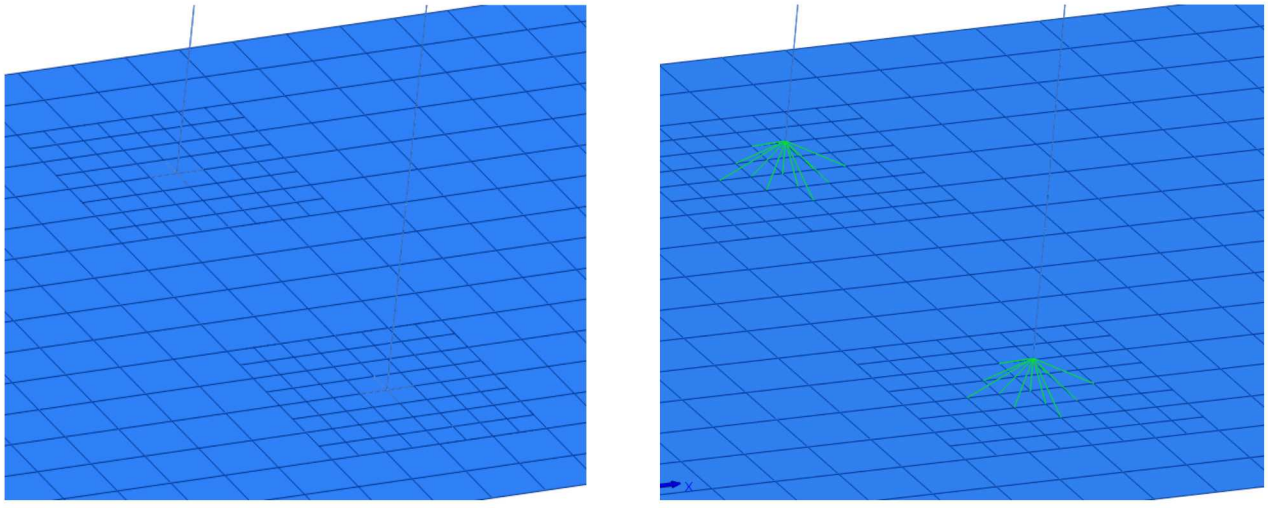

Figure 6. Comparison of joint modeling techniques in the two models developed, the first (left) directly connecting the beam element to a plate element node, and the second (right) using rigid elements to cover the area corresponding to the cap nut.

Table 1. Correlation of selected finite element modes with measured experimental mode

FEA	Freq. (Hz)	EMA	Freq. (Hz)	Diff. (%)	MAC (%)	POC (%)
1	96.933	1	85.197	13.77	98.9	99.7
2	155.52	2	151.07	2.94	99.4	99.8
3	199.16	3	189.1	5.32	98.3	99.3
4	262.88	4	257.07	2.26	99.1	99.8
5	282.69	5	261.22	8.22	96.8	99.2
6	422.62	6	413.76	2.14	98.8	99.5
9	555.55	7	487.55	13.95	96.9	98.5
7	518.25	8	509.08	1.8	76.1	96.4
9	538.84	9	513.77	4.88	97.4	91.3
8	549.84	10	540.05	1.81	13.6	83.6
11	678.5	11	608.52	11.5	98.4	99.8
12	743.8	12	690.98	7.64	98.3	98.9
13	877.86	13	744.65	17.89	94.5	94.8

ANALYTICAL TEST CASES

Prior to applying these techniques experimentally, three analytical test cases were studied. The first test case was used to validate the force reconstruction process for the structure being tested, without introducing any gap contact. The second was used to show the extension of the force reconstruction process for multiple uncorrelated inputs to the structure that occur at different times and locations. The third case demonstrated how the force reconstruction process was altered to incorporate the composite locator for the internal, correlated forces that the structure would experience if nonlinear gap impacts occurred.

- Analytical Case 1: Reconstruction of a single input
- Analytical Case 2: Reconstruction of multiple *uncorrelated* inputs
- Analytical Case 3: Reconstruction of multiple *correlated* inputs

A modal damping of 4% was assumed over all modes, and the physical response for all three cases was calculated by performing a direct integration of the equations of motion using the Newmark-β integration technique [11].

Analytical Case 1: Reconstruction of a Single Input

The force reconstruction technique was applied to the structure when excited by a 20 ms wide sine burst, shown in Figure 7. The excitation was applied at DOF# 8583 of the finite element model, which is to the right of the midpoint of the outer surface of one of the beams. This is the same location that was used as the shaker input for the experimental work.

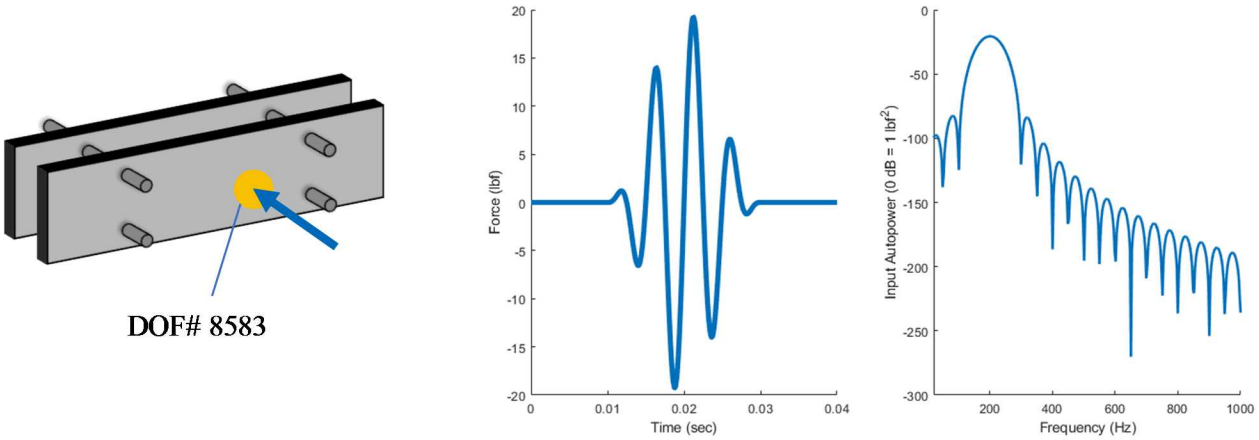

Figure 7. Force pulse applied to the structure (left) in the time (center) and frequency (right) domains.

The modal responses for the first thirteen modes were estimated using the pseudoinverse of the mode shape matrix. The modal forces were estimated from the modal response coordinates using the inversion of the FRF matrix as described in Eq. 6. For brevity, these are not shown.

A singular value decomposition was performed to decompose the modal force vectors, as shown in Eq. 7. One significant singular value was identified and the associated singular vector was used as a truncated basis. The modal coefficients of each degree of freedom were projected onto this truncated basis to calculate the primary locator function, which correctly identified DOF# 8583 as the location of the force input. The singular value decomposition and the primary locator function are shown in Figure 8.

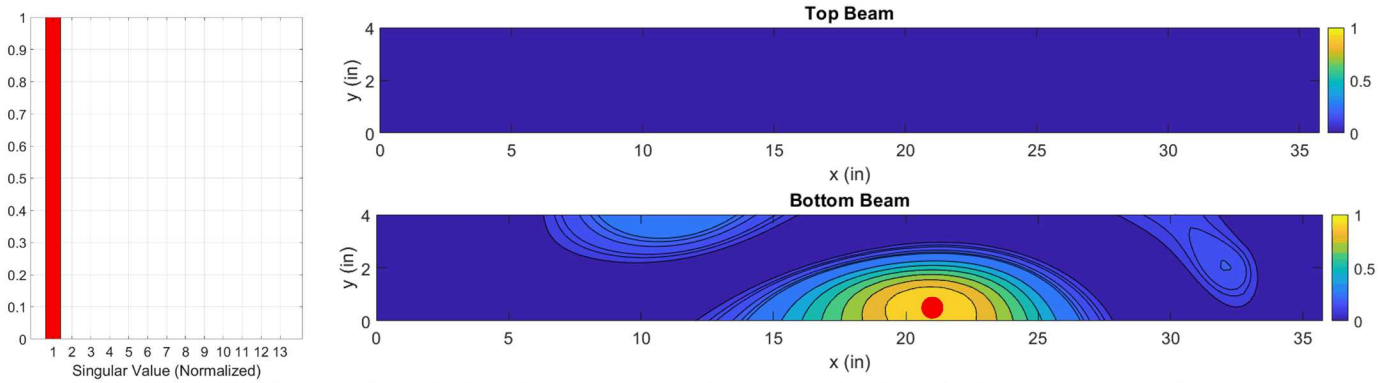

Figure 8. Singular value decomposition (left) and primary locator function (right) for a single input acting on the structure.

The modal forces were projected back to physical space and compared to the original input in both the time and frequency domains, shown in Figure 9. The estimated input matches the applied input very well in both the frequency domain and time domain, demonstrating that the force reconstruction process was able to accurately estimate the applied force for the case of a single localized input on the structure.

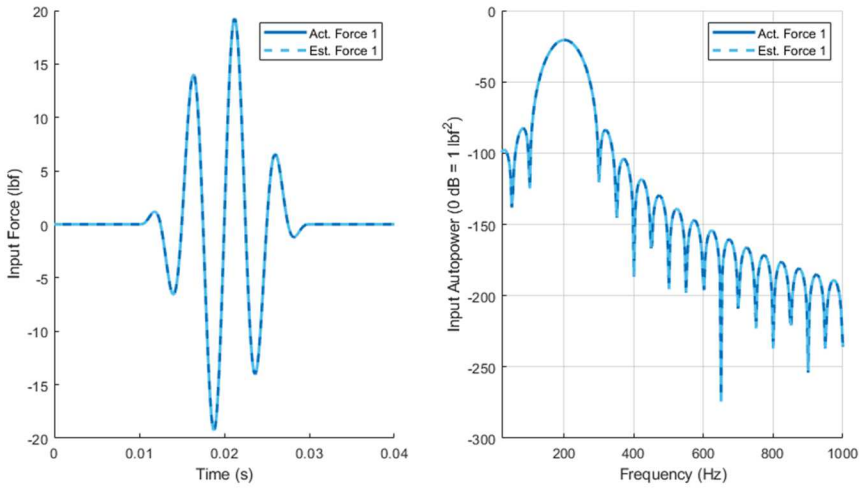

Figure 9. Estimated input force compared to the actual input force in the time domain (left) and frequency domain (right).

Analytical Case 2: Reconstruction of Multiple Uncorrelated Inputs

The structure was excited by three forces, a 20 ms wide sine burst at DOF# 8583 and two 1 ms wide half sine pulses at DOFs# 291 and 14979. The half sine pulses, which were equal in magnitude and opposite in direction of application, were chosen to approximate the shape of the force the structure would experience if subjected to nonlinear gap contacts. However, the two half sine pulse inputs occurred at different points in time, such that no forces were correlated. The excitation is shown in Figure 10. The physical response was calculated, and modal responses and modal forces were estimated using the first thirteen modes of the structure.

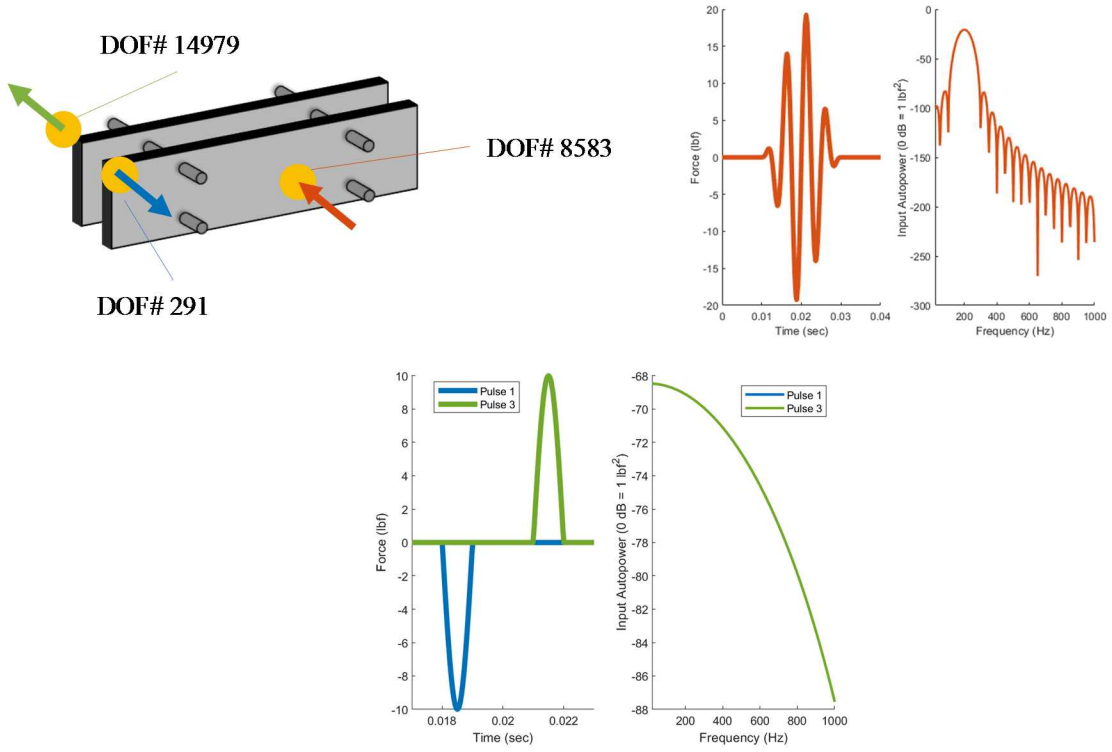

Figure 10. Structure excited by three forces (top left): a sine burst (top right) applied at DOF# 8583 and two equal but opposite and temporally-separated half sine pulses (bottom) applied at DOF# 291 (blue) and DOF# 14979 (green).

A singular value decomposition of the estimated modal forces provided three dominant singular values. Localization with the three dominant singular vectors correctly indicated the input locations of all three forces. The singular values and localization are shown in Figure 11.

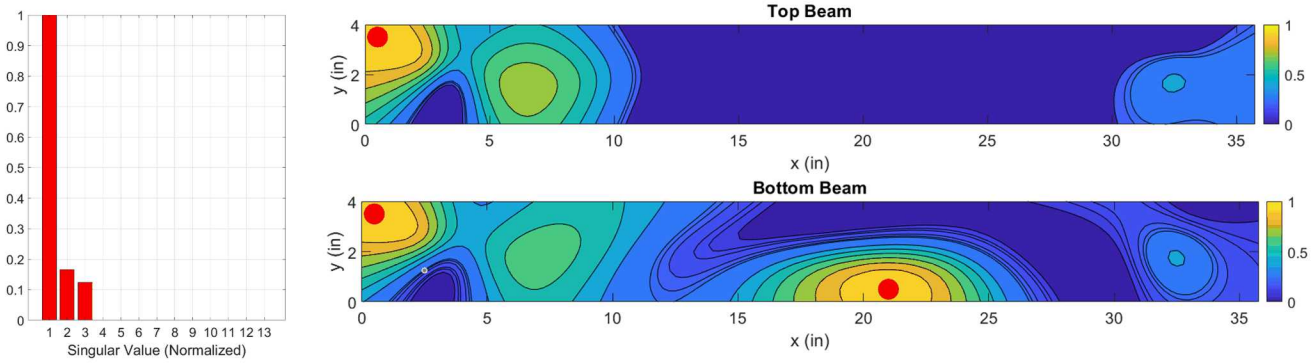

Figure 11. Singular values (left) and primary locator function (right) with red markers indicating the correct input locations

The estimated modal forces were projected back to physical space at the DOFs indicated by the primary locator function, DOFs# 291, 8583, and 14979. The estimated forces correspond very well with the original input forces, as shown in Figure 12, indicating that the force reconstruction process can be extended to cases where a system is subjected to multiple uncorrelated inputs.

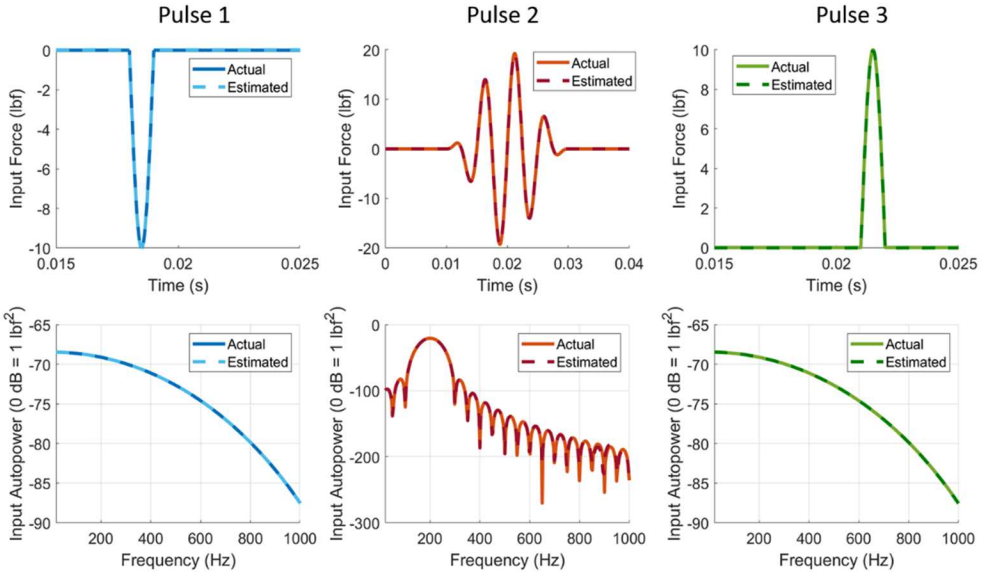

Figure 12. The estimated input forces compared with the actual input forces in the time domain (top) and frequency domain (bottom).

Analytical Case 3: Reconstruction of Multiple Correlated Inputs

The structure was excited by the same three forces as in the previous case, (a 20 ms wide sine burst at DOF# 8583 and two 1 ms wide half sine pulses at DOFs# 291 and 14979). However, for this case, the two half sine pulse inputs occurred simultaneously, resulting in correlated forces. This allows for insight into how the force reconstruction process performs on a structure that experiences nonlinear gap contact behavior producing correlated force inputs. The physical response was calculated, and modal responses and modal forces were estimated using the first thirteen modes of the structure. A singular

value decomposition of the estimated modal forces provided two dominant singular values. While three forces were applied to the model, the two correlated forces are regarded as a single principal force component by the singular value decomposition process, resulting in one singular value for the sine burst input and a second singular value for the two correlated half sine pulses.

The uncorrelated force was located by using the two significant singular vectors to calculate the primary locater function, shown in Figure 13. The red markers on the plot show the actual force input locations, while the colormap shows the primary locator values. The uncorrelated force was correctly located at (21,0.5) on the bottom beam. Predictably, the locations of the correlated forces were not detected using primary locator function. These results could be used to reconstruct the uncorrelated force individually, but the correlated forces would not be estimated. In order to perform reconstruction for all three forces accurately, the correlated forces need to be located using the composite locator function, then the results from the two locater functions can be combined for the estimation process.

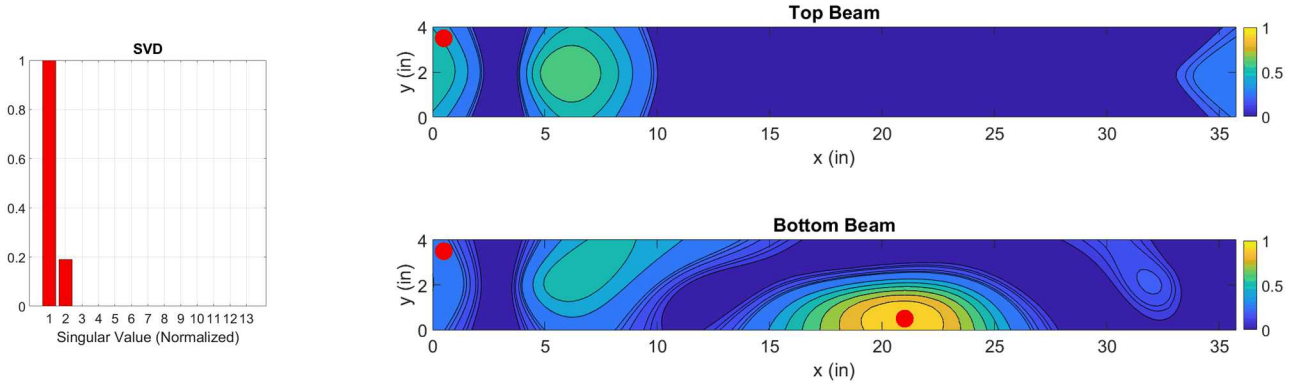

Figure 13. Singular values (left) and primary locator function (right) with red markers indicating the correct input locations.

To supplement the results of the primary locator function, a composite locator function was computed from Eq. (13). Node pairs were generated for each x-y coordinate pair, such that for a given node from the bottom beam with coordinates x1, y1, the corresponding paired node was located on the top beam, also with coordinates x1, y1. Where the primary locator function of the prior section contained values for 5606 individual nodes, the composite locator function under consideration provided values for 2803 node pairs. From the composite locator function described, the pair of DOFs that corresponded to the input locations of the correlated input were correctly located, as shown in Figure 14. Note that the composite locator function did not locate the uncorrelated force applied to the structure, so the results from the primary locator and the composite locator need to be combined for the final estimation process.

While the composite locator function correctly identified the input pair of DOFs, there appears to be less precision in the location in the y-dimension, seen by the lack of contour lines. This is likely to be due to the nature of the modes used in the reconstruction efforts. For the majority of the modes considered, the differences between the modal coefficients of the nodes of the top beam and the corresponding nodes of the bottom beam were approximately uniform in the y direction. For these modes, application of equal but opposite forces to the node pairs considered would result in almost constant modal force along the y direction. Thus, for the modes considered, the structure is not generally sensitive to movement of the contact location in the y direction. Only a small number of modes feature slight torsional behavior, such that, in considering the anticipated contact forces, these modes would be sensitive to changes in the y direction. Therefore, the low y sensitivity observed in the composite locator function appears to be a consequence of the structure used, rather than the function itself. Despite the relative insensitivity, the results indicate that correlated inputs similar to those expected from nonlinear gap contacts can be correctly located using the composite locator function.

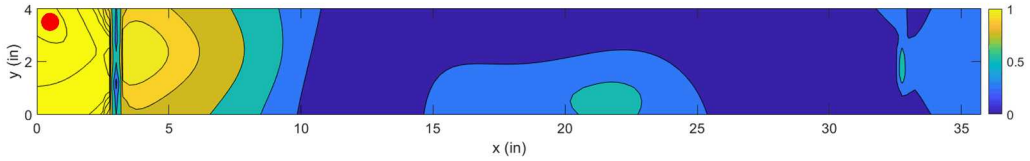

Figure 14. The composite locator function, with the pair of DOFs associated with the correlated force inputs correctly identified

The applied forces were estimated with the force estimation process described in Eq. (9), combining the input DOF located with the primary locator function and the composite locater function. The resulting estimated forces are highly accurate and are shown in Figure 15. While formulating the composite locator does require additional assumptions, with sufficient knowledge of the structure of interest and the desired application correlated forces can be located to supplement the results of the primary locater for the force estimation process. This two-step procedure results in highly accurate reconstructed forces and expands the potential applications for the technique.

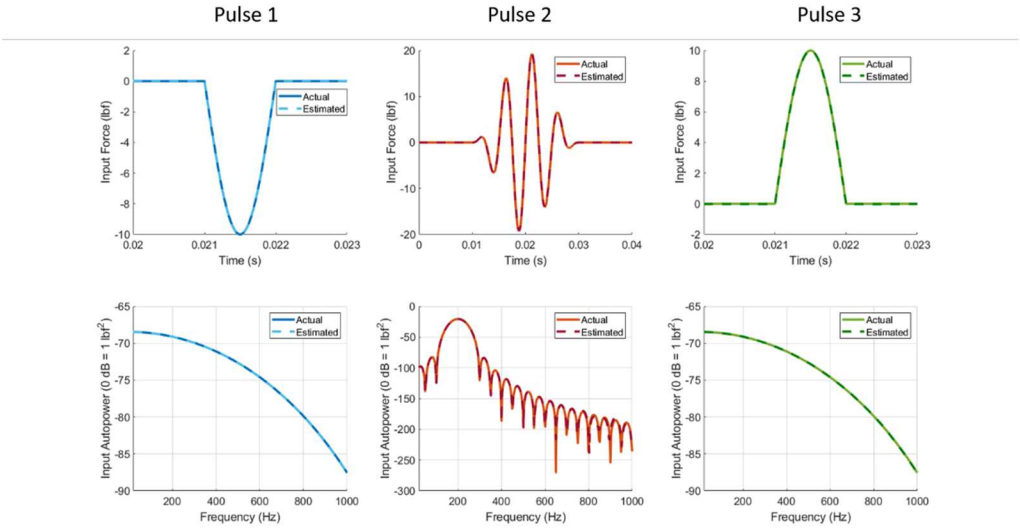

Figure 15. The estimated input forces compared with the actual input forces in the time domain (top) and frequency domain (bottom).

EXPERIMENTAL TEST CASES

To show the technique experimentally, four cases were completed. Case 1 show the reconstruction of the response of the linear system, absent any intermittent contact, to a hammer impact, which is similar to results presented in [7]. Case 2 demonstrated the results of reconstructing a nonlinear gap contact force. Cases 3 and 4 used force reconstruction to quantify the stiffness change of one and two preloaded contact points, respectively. These cases present dynamics that are similar to the effect of a loosened bolt and provide insight to this potential application. Cases 2, 3, and 4 use shaker excitation and are excited using a short sine burst at 85 Hz, which is the natural frequency of the first bending mode of the system.

- Experimental Case 1: Linear Response to Hammer Impact
- Experimental Case 2: Nonlinear Gap Impact
- Experimental Case 3: One Preloaded Contact Point
- Experimental Case 4: Two Preloaded Contact Points

Several metrics were considered to determine the accuracy of the experimental results. For localization, the absolute distance between the estimated location of the force and the known input of the force were used, as well as a percent error calculation where this distance was compared to the longest dimension of the structure. Estimated forces were evaluated in both the time and frequency domains using the TRAC and FRAC respectively, compared to the force data acquired from the force gauges at each force location. The primary focus of this experimental exploration is to determine if the technique can be extended to identification and characterization of phenomena associated with bolt loosening, such as nonlinear contact and change in joint stiffness. To this end, data such as modal estimates, frequency lines, and singular values were excluded where they were known to carry significant error. Metrics for selecting or rejecting data is a topic for further development and is outside the scope of this work.

Experimental Case 1: Linear Response to Hammer Impact

For Case 1, a force was applied to the structure via a soft plastic tipped modal hammer impact at measurement point 13, which was approximately midspan on the bottom beam and located near the edge, so as to excite both bending and torsion modes.

None of the contact points were engaged, resulting in a linear system. Localization was performed using a frequency bandwidth from 200 to 400 Hz and modes 1, 2, 5, 6, 8, 9, 10, 11, and 12. The resulting normalized singular values were shown in Figure 16, with the primary locator plotted in the color map. A single significant singular value was identified and used in the calculation of the primary locator function. The primary locator function was able to correctly identify the impact location within 0.25 inches, or 0.7% of the diagonal length of the beam. Note that, as with the analytical cases, the input location is indicated on the primary locator function using a red marker.

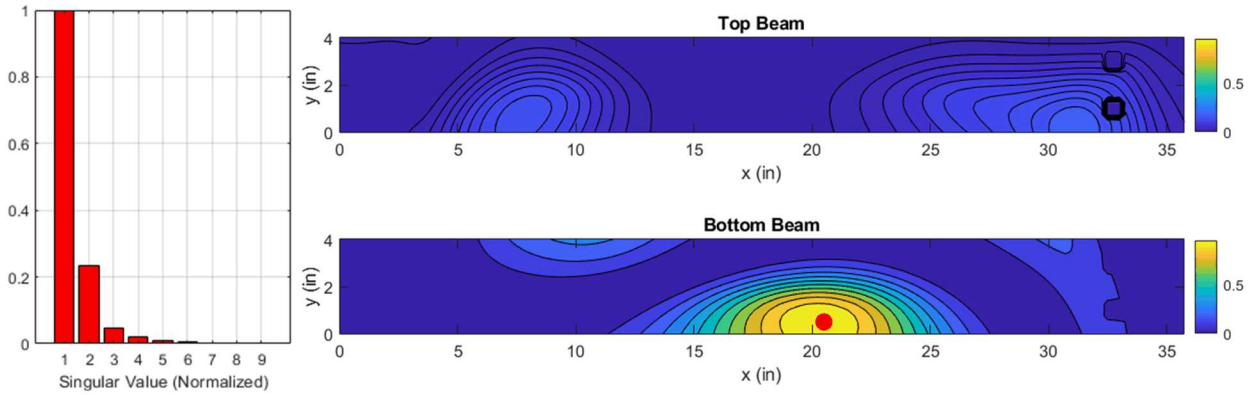

Figure 16. Singular Value Decomposition and Primary Locator Function for Hammer Impact

The force reconstruction process was used to recreate an estimate of the input force in both the time and frequency domains, as shown in Figure 17. Frequency content between 40 to 250 Hz from modal estimates 1, 2, and 5 was included. The input force was very well reconstructed in the frequency domain. The time domain reconstruction matches the amplitude and shape of the applied input as well, with some slight discrepancies due to truncation of frequency domain information prior to the transformation to the time domain.

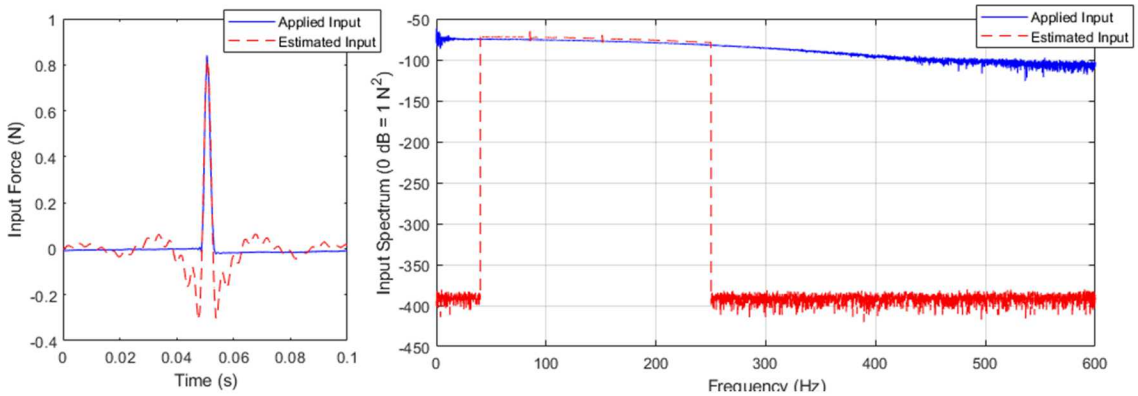

Figure 17. Force Reconstruction in Time and Frequency Domain of Hammer Impact

Experimental Case 2: Nonlinear Gap Impact

For Case 2, shaker excitation was used with one of the contact points engaged with a gap height of 0.0027 inches (shown in Figure 18) so that when the structure was excited the bolt and force gauge would impact, resulting in a nonlinearity. The estimated forces were then compared to measured data recorded by the force gauge.

Figure 18. Close-up picture of the nonlinear gap that acts as a contact point when the structure is excited

Localization of the shaker input was performed using a frequency bandwidth of 65 to 531 Hz and mode shapes 1, 2, 5, 6, 8, 9, 10, 11, and 12. The resulting normalized singular values are shown in Figure 19 along with resulting primary locator function where the three most significant values were used. The primary locator function was able to locate the shaker input within 0.5 inches, or 1.4% error. However, the nonlinear gap impact forces were not located using the primary locator function, as predicted from the analytical case studies.

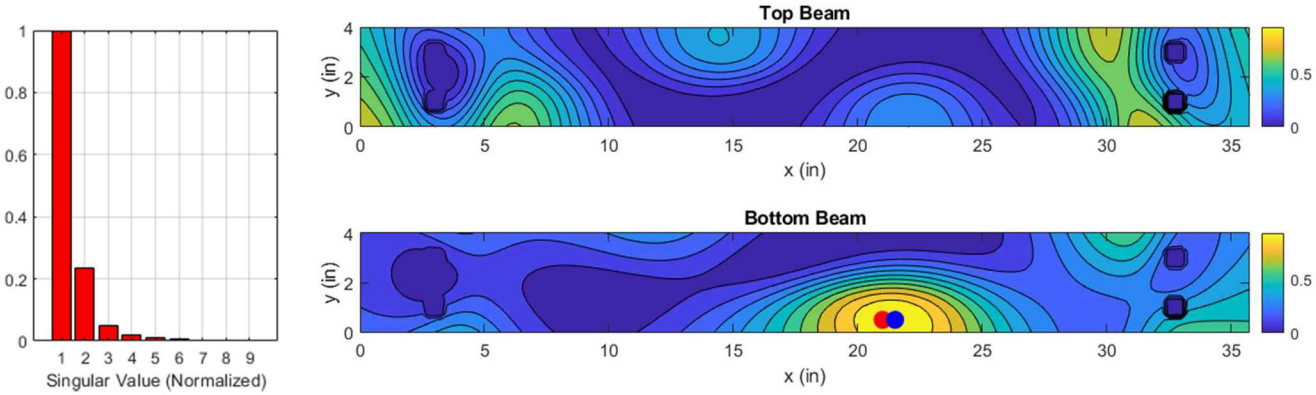

Figure 19. Singular Value Decomposition and Primary Locator Function of Shaker Excitation

The resulting reconstruction of the shaker force that used frequencies from 40 to 460 Hz and mode shapes 1,2, and 5 is shown in Figure 20 for both the frequency and time domains. For this extended shaker burst, the reconstruction process was able to achieve high correlation to the measured input values with respect to both the time and frequency domains. For this reconstruction the TRAC value was 99%, and the FRAC value was 99.8%, indicating very high correlation and an accurate reconstruction for frequency range considered.

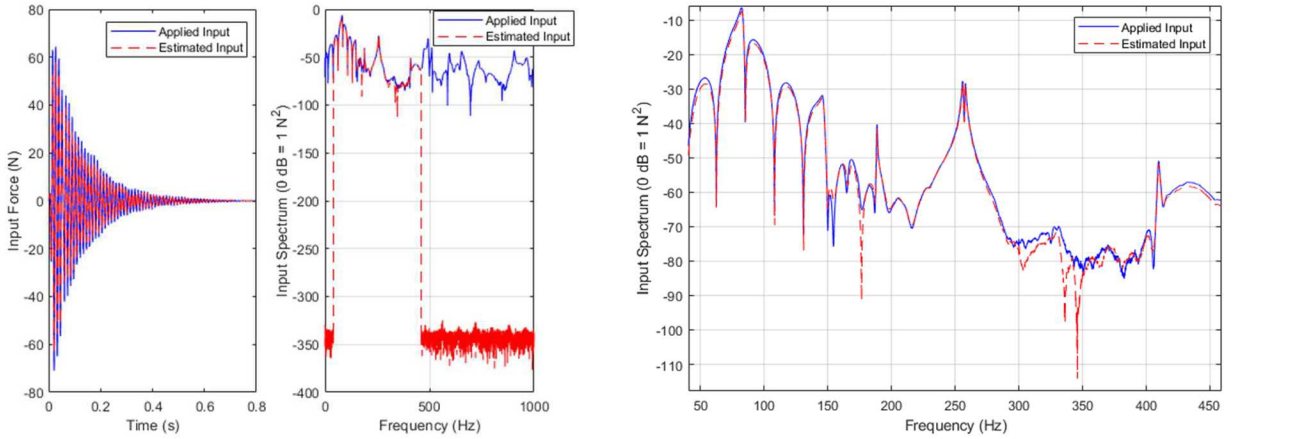

Figure 20. Force Reconstruction in the Time and Frequency domains for the shaker in the case of the nonlinear gap impact

The nonlinear contact point was then located using the Composite Locator Function. Two significant singular values from the singular value decomposition shown in Figure 19 were used in the composite locator function. The result of the composite locator function is shown in Figure 21, where the estimated location is within 0.5 inches of the actual input, or 1.4% error.

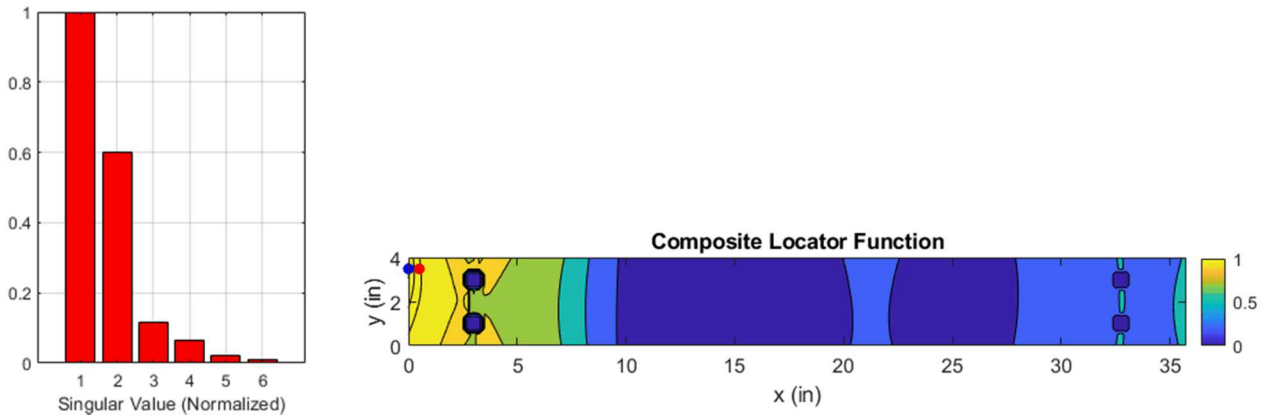

Figure 21. Composite Locator Function used to locate where the nonlinear gap impact is occuring. The red marker is the nonlinear gap impact location, and the blue marker is the estimated location.

Force reconstruction was then performed on the gap contact point using frequencies from 147.5 to 637.5 Hz, and mode shapes 1, 2, 5, and 12. The results for the top and bottom beams are shown in Figure 22. As with the hammer impact, the reconstruction of the frequency domain is very accurate, while in the time domain there is some error resulting from frequency domain truncation. The TRAC values are 53% and 57% for the top and bottom beam reconstructions respectively, while the FRAC values are 95% for the top beam and 99% for the bottom beam.

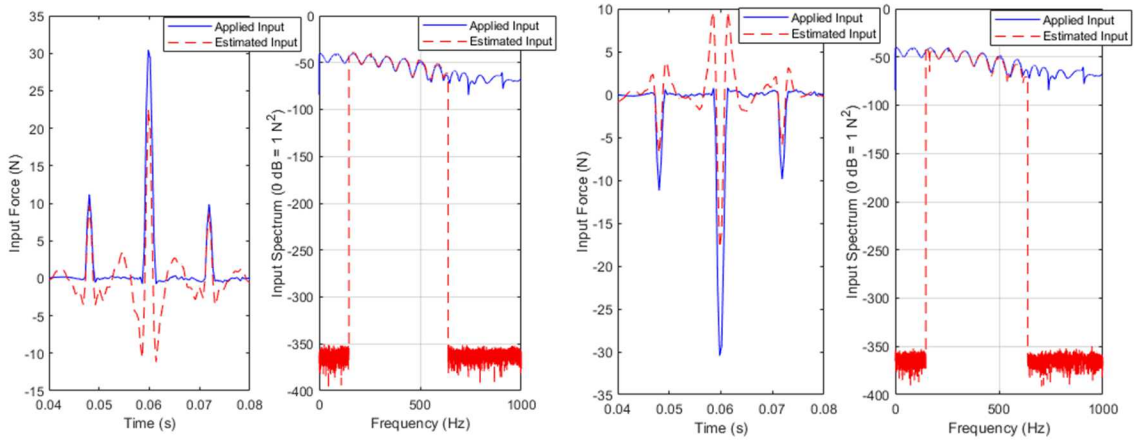

Figure 22. Force Reconstruction in the time and frequency domains of the nonlinear gap impact for the top (left) and bottom (right) beams

Experimental Case 3: One Preloaded Contact Point

For Case 3, one of the contact points was engaged such that the set screw was in contact with the force gauge as shown in Figure 23, so that there was a slight preload in the connection. The preload did not effect the time or frequency response data as long as the combined forces of the excitation and preload are not greater than the range of the gauge. This case is similar to a joint where a bolt has loosened and lost some of its preload in that the condition represents a change in stiffness.

Figure 23. Close-up picture of the nonlinear preloaded contact point

The primary locator function was used to locate the shaker input force using a frequency band from 250 to 281 Hz and mode shapes 1, 3, 4, 5, and 12. The resulting singular value decomposition provided two singular values that were used to locate the shaker impact site, shown in Figure 24 along with the primary locator function. The primary locator function was able to estimate the actual applied input within 0.57 inches or 1.6% error.

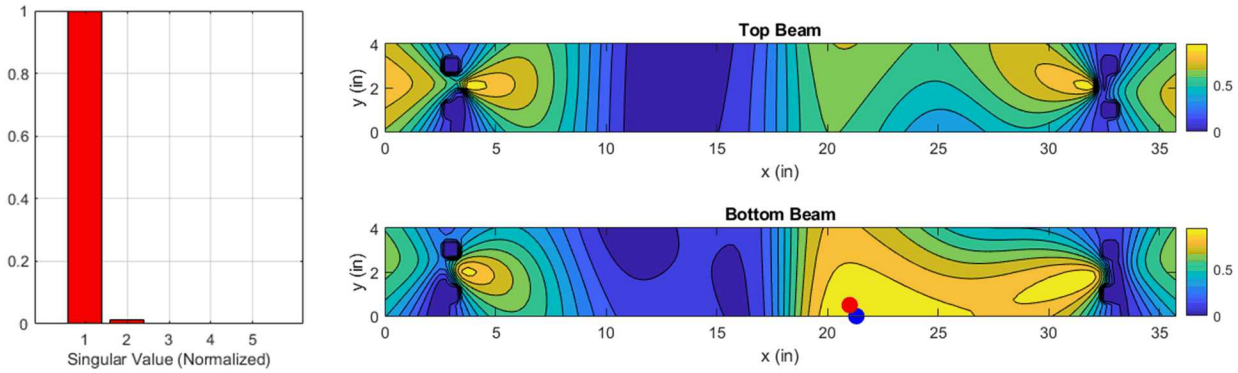

Figure 24. Singular Value Decomposition and Primary Locator Function for the shaker input force for Case 3

Using the location estimated with the primary locator function, a frequency band from 62.7 to 281.4 Hz, and mode shapes 1, 6, 8, and 11, the shaker force was reconstructed accurately, detailed in Figure 25. The reconstruction in both the time and frequency domains were very well correlated in amplitude and shape. Both the TRAC and FRAC values for this reconstruction are 98%.

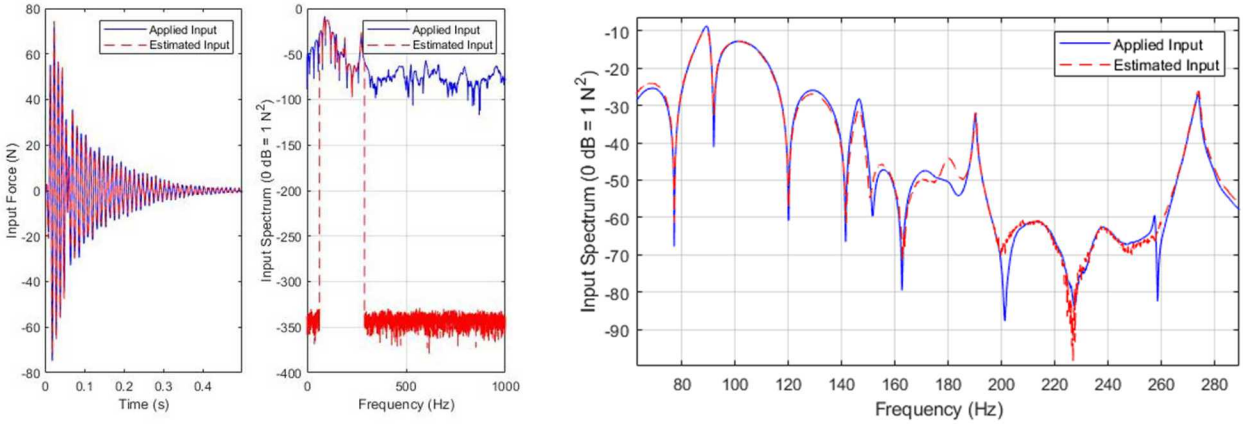

Figure 25. Force Reconstruction in the time and frequency domains for the shaker input Case 3

The composite locator function was then used to locate the preloaded contact point. Frequency content from 272 to 278.1 Hz and mode shapes 1, 2, 3, 5, 7, 8, 10, and 12 were used in the singular value decomposition, shown in Figure 27. One significant singular value was identified and used to calculate the composite locator function, shown in Figure 27. The estimated location is 1.5 inches from the actual contact point, or 4.2% error. Most of this discrepancy is along the shorter length of the beam. The dynamics of the test structure in the frequency range studied include minimal torsional behavior, resulting in difficulties distinguishing along the shorter dimension of the beam.

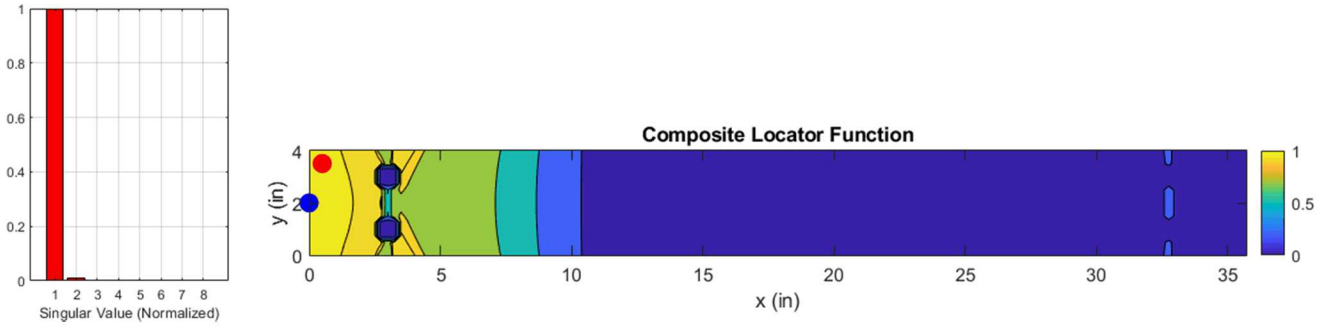

Figure 26. Singular Value Decomposition and Composite Locator Function for the preloaded nonlinear contact point

Using the estimated location, frequencies from 70.5 to 125.1 Hz, and mode shapes 1, 2, 4, 5, and 10, the reconstruction was performed for the preloaded contact point, resulting in the very accurate force reconstructions shown in Figure 27. For the top beam, the TRAC and FRAC values are 97% and 99% respectively, and for the bottom beam the TRAC and FRAC values are 98% and 99% respectively. The preloaded contact point was reconstructed with higher accuracy when compared to the nonlinear gap contact case, likely due to the more limited frequency range excited by the preloaded contact point.

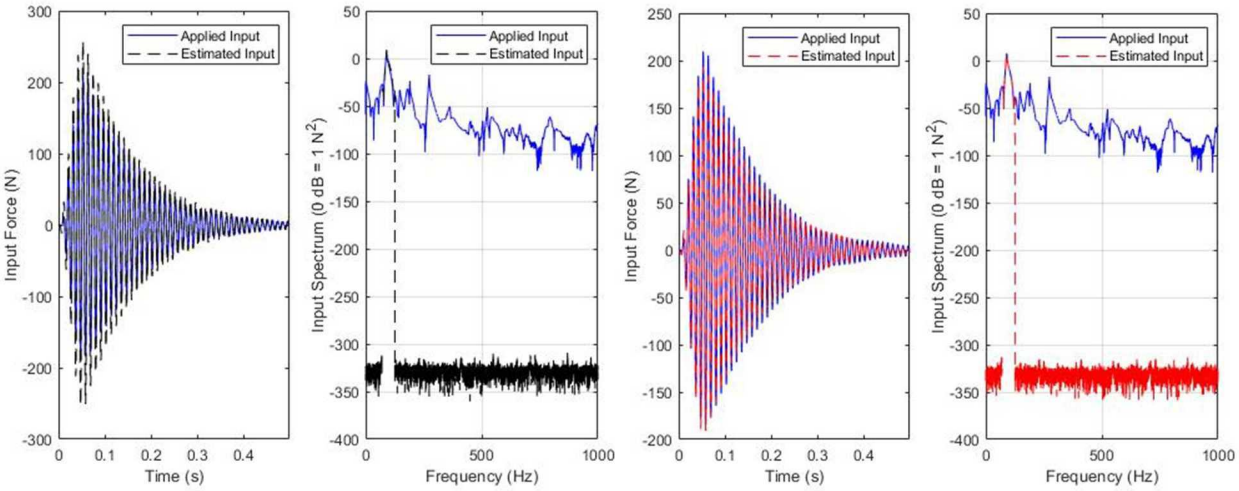

Figure 27. Force Reconstruction in the time and frequency domains of the preloaded nonlinear contact point for the top (left) and bottom (right) beams

Experimental Case 4: Two Preloaded Contact Point

The final case that was studied was an extension of the previous case, using two preloaded points located on opposite corners of the structure. Both preloaded contact points are engaged as detailed in Case 3 and shown in Figure 23.

The primary locator function was used to locate the shaker input using a frequency band from 62.6 to 281.4 Hz, and mode shapes 1, 2, 3, 4, 9, 10, 11, and 12. The resulting singular value decomposition is shown in Figure 28 along with the primary

locator function, calculated using 3 singular values. The estimated shaker force input location was 0.39 inches away from the actual input site, or 1.1% error. The estimated shaker location is shown as a blue marker, and is the maximum value of the primary locator.

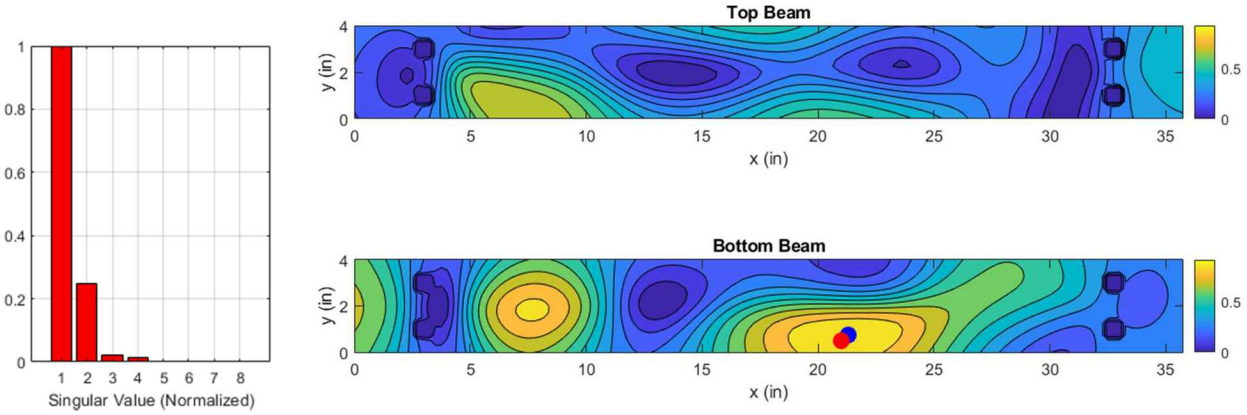

Figure 28. Singular Value Decomposition and Primary Locator Function for the shaker input force in Case 4

Force reconstruction of the shaker input was performed using frequency bands from 62.7 to 281.4 Hz, and mode shapes 1, 2, 3, 4, 9, 10, 11, and 12. The results of this reconstruction are shown in Figure 29 and are highly accurate, with a TRAC value of 95% and a FRAC value of 97%.

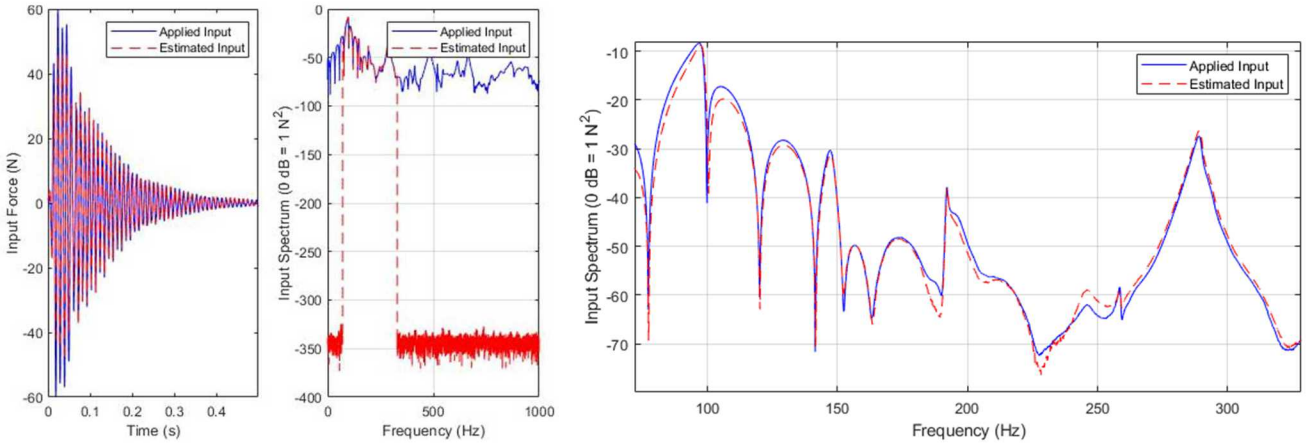

Figure 29. Force Reconstruction in the time and frequency domains for the shaker input in Case 4

To locate the two pairs of correlated forces, a singular value decomposition was performed using frequencies from 281.4 to 297 Hz and mode shapes 1, 3, 5, 6, 8, and 12, shown in Figure 30. The composite locator function was calculated using two singular values and the estimated locations of the two preloaded locations are shown in Figure 30. The estimated location of the contact point in the top left corner of the composite locator function was 0.5 inches away from the actual contact location, or 1.4% error. The estimated location of the contact point in the bottom right corner of the composite locator function was 1.5 inches from the actual contact point, or 4.2% error. This error in the short dimension of the beams is similar to the error seen previously in Case 3.

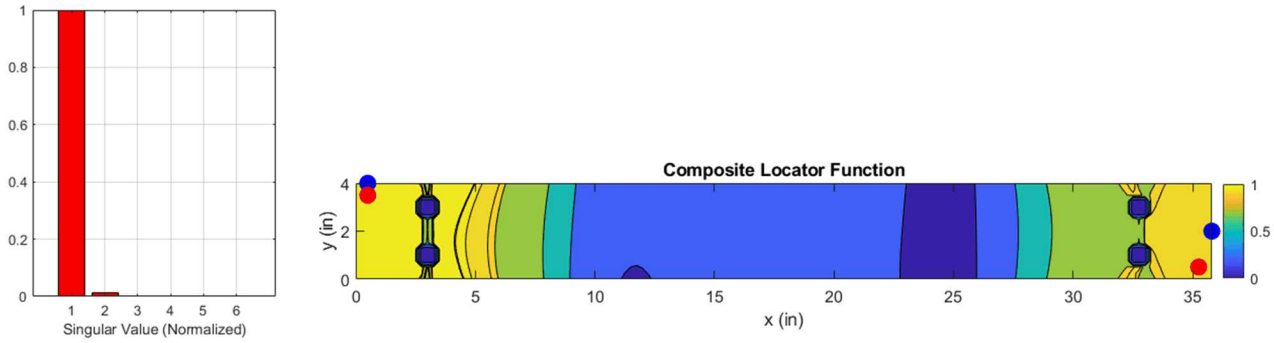

Figure 30. Singular Value Decomposition and Composite Locator Function for the two preloaded nonlinear contact points

Figure 31 and Figure 32 show the force reconstruction of preloaded contact point that can be found in the top left and bottom right of the plot in Figure 30, respectively. This reconstruction used frequencies from 78.3 to 125.1 Hz, and mode shapes 1, 2, and 7.

Figure 31 shows the reconstruction of the bottom right contact point. The force applied to the top beam of the structure had both a TRAC and FRAC value of 98%. The force applied to the top beam of the structure also had a TRAC value of 98% and FRAC value of 98%. Both points were reconstructed with a high degree of accuracy.

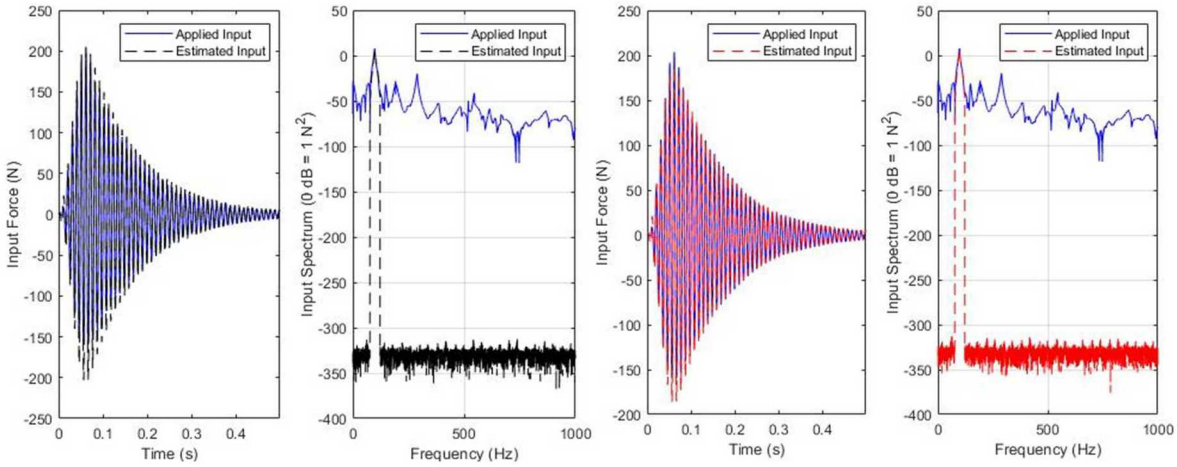

Figure 31. Force Reconstruction in the time and frequency domains of the bottom right preloaded contact point for the top (left) and bottom (right) beams

Figure 32 similarly shows the reconstruction of the preloaded contact point found in the top left of Figure 30 for the top and bottom beams. The reconstruction for the top beam had a TRAC and FRAC values of 99%. The reconstruction for the bottom beam also had TRAC and FRAC values of 99%. These results show that the stiffness changed due to a preloaded contact point can be reconstructed with a high level of accuracy, and indicate that these methods could be used in future work to identify loosened bolts.

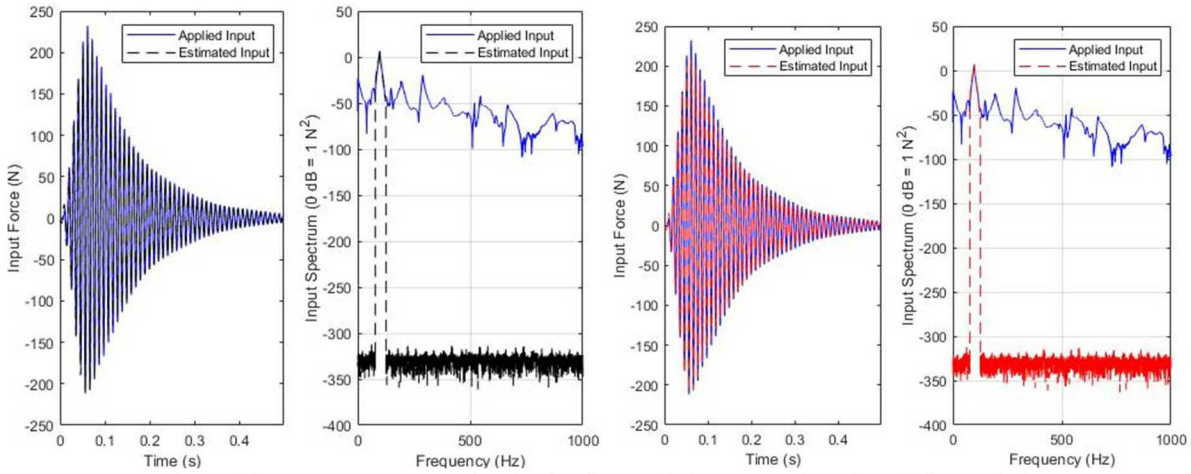

Figure 32. Force Reconstruction in the time and frequency domains of the top left preloaded contact point for the top (left) and bottom (right) beams

CONCLUSION

Several analytical cases were presented to demonstrate the need to modify the force reconstruction process to accommodate correlated forces. The composite locator function was presented and used in several analytical and experimental cases to demonstrate the accuracy of the technique. While the composite locator involves more assumptions than the primary locator and is therefore more limited in scope, the function allows for the accurate localization of correlated forces. While the correlated forces studied in this work focused on internal reaction forces such as nonlinear gap contact and preloaded connections, this technique could also be applied to distributed loading, external correlated inputs, and distributed system changes such as a global stiffness change due to a deformation. Using the primary locator to identify uncorrelated forces then supplementing this with the composite locator constructed using foreknowledge of the structure at hand allows for a complete characterization of applied forces, nonlinear behavior, and system changes. This work lays the groundwork for a variety of future applications, including system change identification, reconstructing equivalent nonlinear forces from joints, identification of loosened bolts, and structural health monitoring of jointed structures.

ACKNOWLEDGEMENTS

This research was conducted at the 2019 Nonlinear Mechanics and Dynamics Research Institute supported by Sandia National Laboratories and hosted by the University of New Mexico.

Sandia National Laboratories is a multimission laboratory managed and operated by National Technology and Engineering Solutions of Sandia, LLC., a wholly owned subsidiary of Honeywell International, Inc., for the U.S. Department of Energy's National Nuclear Security Administration under contract DE-NA-0003525.

This project is funded by NSF Graduate Research Fellowship Program with Jong-on Hahm, funding number 1656341, and Principal Investigator and Project Advisor Peter Avitabile.

The authors would also like to thank Bill Flynn from Siemens Industry Software NV for supplying the data acquisition systems used to collect the experimental measurements presented throughout this work.

REFERENCES

[1] L. Gaul and J. Lenz, "Nonlinear dynamics of structures assembled by bolted joints," *Acta Mechanica,* vol. 125, no. 1, pp. 169-181, 1997.

[2] L. Gaul and R. Nitsche, "The Role of Friction in Mechanical Joints," *Applied Mechanics Reviews,* vol. 54, no. 2, pp. 93-109, 2001.

[3] S. Bograd, P. Reuss, A. Schmidt, L. Gaul and M. Mayer, "Modeling the dynamics of mechanical joints," *Mechanical Systems and Signal Processing,* vol. 25, pp. 2801-2826, 2011.

[4] R. Lacayo, L. Pesaresi, J. Groß, D. Fochler, J. Armand, L. Salles, C. Schwingshackl, M. Allen and M. Brake, "Nonlinear modeling of structures with bolted joints: A comparison of two approaches based on a time-domain and frequency-domain solver," *Mechanical Systems and Signal Processing,* vol. 114, pp. 413-438, 2019.

[5] D. J. Segalman, D. L. Gregory, M. J. Starr, B. R. Resor, M. D. Jew, J. P. Lauffer and N. M. Ames, "Handbook on dynamics of jointed structures, Tech. Rep. SAND2009-4164," Sandia National Laboratories, Albuquerque, NM, 2009.

[6] Q. Zhang, R. Allemang and D. Brown, "Modal filter: Concept and applications," in *The 8th International Modal Analysis Conference*, Kissimmee, FL, 1990.

[7] P. Logan and P. Avitabile, "Impact reconstruction Using Modal Filters," in *The 36th International Modal Analysis Conference*, Orlando, FL, 2018.

[8] P. Logan, D. Fowler and P. Avitabile, "Validation of Force Reconstruction for Linear and Nonlinear System Response," in *The 37th International Modal Analysis Conference*, Orlando, FL, 2019.

[9] P. Logan, A. Avitabile and J. Dodson, "Reconstruction of External Forces Beyond Measured Points Using a Modal Filtering Decomposition Approach," *Experimental Techniques,* pp. 1-13, 2019.

[10] P. Avitabile, *Modal Model Correlation Techniques,* Lowell, MA: University of Massachusetts Lowell, 1998.

[11] N. M. Newmark, "A method of computation for structural dynamics," *Journal of the Engineering Mechanics Division,* vol. 85, no. 3, pp. 67-94, 1959.